SAND2017-4252R

VSL-1701

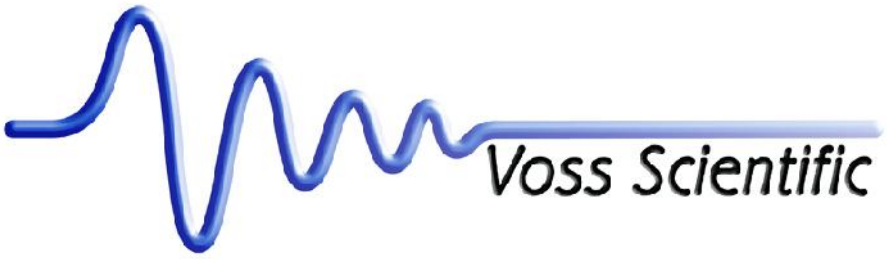

Theory and Circuit Model for Lossy Coaxial Transmission Line

T. C. Genoni, C. N. Anderson, R. E. Clark, J. Gansz-Torres, D. V. Rose and D. R. Welch

March 2017

Prepared for: **Sandia National Laboratories**
Attn: Mark Kiefer

Under Contract: **DE-AC04-94AL85000**

Prepared by: **Voss Scientific, LLC**
418 Washington Street, SE
Albuquerque, NM 87108
www.vosssci.com
(505) 255-4201

THEORY AND CIRCUIT MODEL FOR LOSSY COAXIAL TRANSMISSION LINE

T.C. Genoni, C.N. Anderson, R.E. Clark, J. Gansz-Torres, D.V. Rose, D.R. Welch

Voss Scientific, LLC, 418 Washington ST SE, Albuquerque NM 87108

Abstract:

The theory of signal propagation in lossy coaxial transmission lines is revisited and new approximate analytic formulas for the line impedance and attenuation are derived. The accuracy of these formulas from DC to 100 GHz is demonstrated by comparison to numerical solutions of the exact field equations. Based on this analysis, a new circuit model is described which accurately reproduces the line response over the entire frequency range. Circuit model calculations are in excellent agreement with the numerical and analytic results, and with finite-difference-time-domain simulations which resolve the skin-depths of the conducting walls.

I. Introduction:

Previous work has highlighted the need for models that accurately describe the frequency dependent attenuation of signals propagating in transmission lines with finite conductivity walls [1]. A number of authors have used field analysis to investigate the impedance and attenuation in lossy coaxial lines [2-5]. The frequency dependence of the impedance poses a difficult numerical challenge for which a number of models have been proposed. These include conformal mapping [1], direct integration of the transmission line equations [6], Laplace transform methods [7], and circuit models [8].

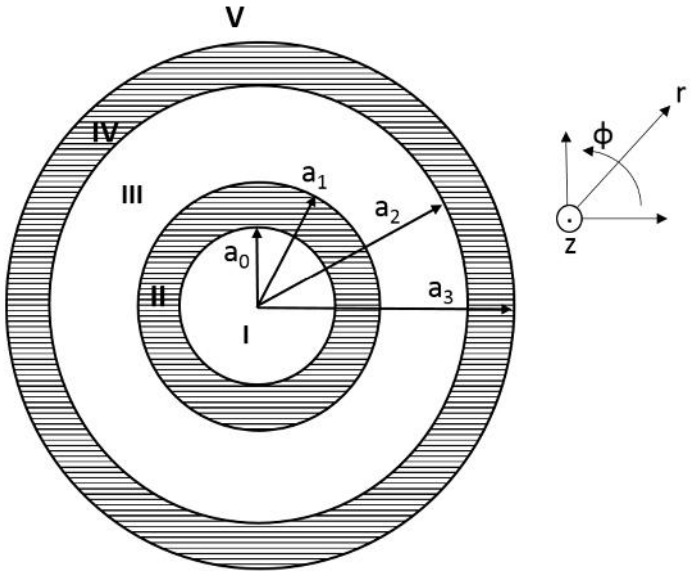

Figure 1. Schematic of coaxial transmission line geometry. Attenuation is due to finite conductivity in conducting regions II and IV.

In this paper we first revisit the theory of the principal transmission line mode in a lossy coaxial line shown schematically in Fig. 1. The principal mode is that with the smallest transverse propagation constant in region III. An early analysis by Schelkunoff [2] treated the case of a solid inner conductor ($a_0 \to 0$) and a finite thickness outer conductor. He assumed negligible displacement currents and equal and opposite conduction currents in regions II and IV, and zero magnetic field outside the outer conductor ($r > a_3$). Under these assumptions, he was able to derive approximate analytic expressions for the surface impedances at $r = a_1$ and $r = a_2$. In his classic text [3], Stratton treated a simpler geometry ($a_0 \to 0$ and $a_3 \to \infty$) and presented expressions for the electric and magnetic fields in regions II, III, and IV. Matching the tangential field components at $r = a_1$ and $r = a_2$ gives a set of equations from which the transverse and longitudinal propagation constants (and hence the longitudinal attenuation constant) can be calculated. Stratton derived approximate formulas for the transverse propagation constant in region III as well as the attenuation constant in the line. Some time later, and under the same simplifying geometry assumptions, Daywitt [4] repeated the field analysis of Stratton and solved the resulting matching equations numerically. He compared his "exact" numerical results to the approximate Stratton formula,

demonstrating its high accuracy from DC up to about 20 GHz. More recently, Gallant [5] used the "surface impedance" concepts employed earlier by Schelkunoff to generalize the Stratton/Daywitt approximate formulas to include the effects of a finite outer conductor. In what follows we generalize the analysis further, taking account of both finite thickness inner and outer conductors. In Sec. 2, we describe the fields in all five regions and present the tangential field matching equations at the boundaries. In Sec. 3, approximate formulas for the propagation constants are derived and shown to reduce to previously presented formulas in the appropriate limits. Accuracy of the new formulas is demonstrated by comparison to numerical solution of the full system of matching equations.

Following this analysis, we propose a new circuit model capable of accurately reproducing the frequency dependent attenuation in a lossy coaxial line from DC to 100 GHz. In Sec. 4 we give details of the circuit model and model parameters corresponding to specific coax parameters are given in Sec. 6. Finite-difference-time-domain (FDTD) electromagnetic simulations which resolve the skin depths of the conductors are described in Sec. 5. In Sec. 6 we discuss the results of the circuit model calculations and compare them to the FDTD simulation results and to the theoretical calculations of Secs. 2 and 3.

2. Field Equations and Matching Conditions:

Making use of Maxwell's equations in the frequency domain,

$$\nabla\times\bar{H} = (\sigma + i\omega\varepsilon)\bar{E}, \tag{1}$$

$$\nabla\times\bar{E} = -i\omega\mu\bar{H}, \tag{2}$$

we write expressions for the azimuthal magnetic field H_ϕ and the longitudinal electric field E_z in each region of the coaxial line. Each field component varies with (z,t) as $e^{i\omega t-\gamma z}$, where the real part of the longitudinal propagation constant γ accounts for the attenuation. For simplicity this factor is omitted in writing the expressions below.

Region I:

$$H_\phi = A_{II} I_1(h_I r) \tag{3}$$

$$E_z = \bar{h}_I A_{II} I_0(h_I r) \tag{4}$$

Region II:

$$H_\phi = A_{21} F_1(h_2 r) + A_{22} F_2(h_2 r) \tag{5}$$

$$E_z = \bar{h}_2 A_{21} F_3(h_2 r) + \bar{h}_2 A_{22} F_4(h_2 r) \tag{6}$$

$$F_1(h_2 r) = K_1(h_2 a_1) I_1(h_2 r) - I_1(h_2 a_1) K_1(h_2 r) \tag{7}$$

$$F_2(h_2 r) = K_1(h_2 a_0) I_1(h_2 r) - I_1(h_2 a_0) K_1(h_2 r) \tag{8}$$

$$F_3(h_2 r) = K_1(h_2 a_1) I_0(h_2 r) + I_1(h_2 a_1) K_0(h_2 r) \tag{9}$$

$$F_4(h_2 r) = K_1(h_2 a_0) I_0(h_2 r) + I_1(h_2 a_0) K_0(h_2 r) \tag{10}$$

Region III:

$$H_\phi = A_{31} I_1(h_3 r) + A_{32} K_1(h_3 r) \tag{11}$$

$$E_z = \bar{h}_3 A_{31} I_0(h_3 r) - \bar{h}_3 A_{32} K_0(h_3 r) \tag{12}$$

Region IV:

$$H_\phi = A_{41} G_1(h_4 r) + A_{42} G_2(h_4 r) \tag{13}$$

$$E_z = \bar{h}_4 A_{41} G_3(h_4 r) + \bar{h}_4 A_{42} G_4(h_4 r) \tag{14}$$

$$G_1(h_4 r) = K_1(h_4 a_3) I_1(h_4 r) - I_1(h_4 a_3) K_1(h_4 r) \tag{15}$$

$$G_2(h_4 r) = K_1(h_4 a_2) I_1(h_4 r) - I_1(h_4 a_2) K_1(h_4 r) \tag{16}$$

$$G_3(h_4 r) = K_1(h_4 a_3) I_0(h_4 r) + I_1(h_4 a_3) K_0(h_4 r) \tag{17}$$

$$G_4(h_4 r) = K_1(h_4 a_2) I_0(h_4 r) + I_1(h_4 a_2) K_0(h_4 r) \tag{18}$$

Region V:

$$H_\phi = A_{51} K_1(h_5 r) \tag{19}$$

$$E_z = -\bar{h}_5 A_{51} K_0(h_5 r) \tag{20}$$

In the above expressions, I and K are modified Bessel functions, and the transverse propagation constants h_i are given by

$$h_i^2 = -¥^2 - \mu^2 «_i \epsilon_i + i\mu «_i ±_i \ , \tag{21}$$

with

$$\bar{h}_i \equiv \frac{h_i}{(±_i + i\mu \epsilon_i)} \ . \tag{22}$$

Equations for the coefficients are obtained by matching H_ϕ and E_z at a_0, a_1, a_2 and a_3:

$$H_\phi(a_0): \quad A_{11} K_1(h_1 a_0) - A_{21} F_1(h_2 a_0) - A_{22} F_2(h_2 a_0) = 0 \tag{23}$$

$$E_z(a_0): \quad \bar{h}_1 A_{11} I_0(h_1 a_0) - \bar{h}_2 A_{21} F_3(h_2 a_0) - \bar{h}_2 A_{22} F_4(h_2 a_0) = 0 \tag{24}$$

$$H_\phi(a_1): \quad A_{21} F_1(h_2 a_1) + A_{22} F_2(h_2 a_1) - A_{31} I_1(h_3 a_1) - A_{32} K_1(h_3 a_1) = 0 \tag{25}$$

$$E_z(a_1): \quad \bar{h}_2 A_{21} F_3(h_2 a_1) + \bar{h}_2 A_{22} F_4(h_2 a_1) - \bar{h}_3 A_{31} I_0(h_3 a_1) + \bar{h}_3 A_{32} K_0(h_3 a_1) = 0 \tag{26}$$

$$E_z(a_2): \quad \bar{h}_3 A_{31} I_0(h_3 a_2) - \bar{h}_3 A_{32} K_0(h_3 a_2) - \bar{h}_4 A_{41} G_3(h_4 a_2) - \bar{h}_4 A_{42} G_4(h_4 a_2) = 0 \tag{27}$$

$$H_\square(a_2): \quad A_{31} I_1(h_3 a_2) + A_{32} K_1(h_3 a_2) - A_{41} G_1(h_4 a_2) - A_{42} G_2(h_4 a_2) = 0 \tag{28}$$

$$E_z(a_3): \quad -\bar{h}_5 A_{51} K_0(h_5 a_3) - \bar{h}_4 A_{41} G_3(h_4 a_3) - \bar{h}_4 A_{42} G_4(h_4 a_3) = 0 \tag{29}$$

$$H_\square(a_3): \quad A_{51} K_1(h_5 a_3) - A_{41} G_1(h_4 a_3) - A_{42} G_2(h_4 a_3) = 0 \tag{30}$$

Equations (23)-(30) are eight linear homogeneous equations for the A_{ij} which can be written in the form

$$\bar{\bar{M}}\,\bar{A} = 0 \ . \tag{31}$$

Setting $det[\bar{\bar{M}}] = 0$ gives an equation from which the transverse propagation constant in region III (h_3) may be determined numerically. We look for the smallest value of h_3, which corresponds to the principal mode. The other *h*'s and ¥ can be calculated from (21) once h_3 is found. The corresponding eigenvector $\bar{A}$ can then be obtained from (31) and the radial profiles of the electric and magnetic fields calculated, if desired. Numerical results for a specific coaxial geometry will be presented in the next section for comparison to approximate closed-form analytic formulas for h_3 and ¥ which are derived there.

3. Approximate Full-Frequency Formulas for h_3 and ¥ :

In deriving approximate formulas for h_3 and ¥ , we invoke the simplifying assumptions made by Schelkunoff (and later Gallant). The displacement current in the conductors is ignored, and we set $H_\square(a_0) = H_\square(a_3) = 0$ (so that the fields in regions I and V are also ignored). This gives $A_{21} = A_{42} = 0$ and Eq. (31) reduces to

$$\begin{bmatrix} F_2(h_2 a_1) & 0 & -1/h_3 a_1 & 0 \\ \bar{h}_2 F_4(h_2 a_1) & -\bar{h}_3 & -\bar{h}_3 \log(h_3 a_1/2) & 0 \\ 0 & \bar{h}_3 & \bar{h}_3 \log(h_3 a_2/2) & -\bar{h}_4 G_3(h_4 a_2) \\ 0 & 0 & 1/h_3 a_2 & -G_1(h_4 a_2) \end{bmatrix} \begin{bmatrix} A_{22} \\ A_{31} \\ A_{32} \\ A_{41} \end{bmatrix} = 0 \ . \tag{32}$$

In Eq. (32) we take

$$h_2 \approx \sqrt{i\mu\kappa_0\pm_2} \ , \tag{33}$$

and

$$h_4 \approx \sqrt{i\mu\kappa_0\sigma_4} \quad . \tag{34}$$

Also, we have used the small argument approximations for I and K with arguments $h_3 a_1$ and $h_3 a_2$. We set $\kappa = \kappa_0$ everywhere for simplicity.

Setting the determinant of the matrix in Eq. (32) equal to zero gives the following approximation to h_3:

$$h_3^2 \approx \hat{h}_3^2 = \frac{-i\mu^2\epsilon_3\kappa_0}{log\left(a_2/a_1\right)}\left[\frac{1}{k_2 a_1}\frac{F_4\left(h_2 a_1\right)}{F_2\left(h_2 a_1\right)} - \frac{1}{k_4 a_2}\frac{G_3\left(h_4 a_2\right)}{G_1\left(h_4 a_2\right)}\right], \tag{35}$$

where

$$k_i = \sqrt{-i\mu\kappa_0\sigma_i} \; ; \quad \text{i = 2,4} \; . \tag{36}$$

Equation (35) is the generalization of the formula on Gallant page 7 (note the difference in sign convention). It represents a new approximation for h_3 which accounts for the finite thickness of both the inner and outer conductors. In the limit as $a_0 \to 0$ we get the Gallant formula on page 7 of Ref. [5], and as $a_3 \to \infty$ we get Stratton Eq. (40) on page 552 and Daywitt Eq. (35). In the high frequency limit

$$h_3^2 \approx \frac{-i}{log\left(a_2/a_1\right)}\left[\frac{1}{k_2 a_1} + \frac{1}{k_4 a_2}\right] \tag{37}$$

which is the usual "microwave approximation". From Eq. (21) we get an approximate formula for the longitudinal propagation constant:

$$\gamma^2 \approx \gamma^{\wedge 2} = -\hat{h}_3^2 - \mu^2\epsilon_3\kappa_0 \quad , \tag{38}$$

where $\hat{h}_3$ is given by Eq. (35).

The accuracy of the new approximate formulas for h_3 and γ [Eq. (35) and (38), respectively] is illustrated in the numerical calculations below. For these calculations, we adopt the following set of geometry and material parameters (refer to Fig. 1):

$$a_0 = 0.6 \text{ cm}, \; a_1 = 0.7 \text{ cm}, \; a_2 = 1.4 \text{ cm}, a_3 = 1.5 \text{ cm}$$

$$\kappa_i = \kappa_0 \text{ ; i=1..5 and } \epsilon_i = \epsilon_0 \text{ ; i=1..5} \tag{39}$$

$$\sigma_2 = \sigma_4 = 5.0\times10^{17} \text{ s}^{-1} \; .$$

The above value of σ is representative of relatively high conductivity metals.

The equation $det[\bar{\bar{M}}] = 0$ was solved numerically for h_3 as a function of frequency for the above parameters. Substitution into Eq. (21) gives the "exact" numerical solution for the attenuation constant $Re(¥)$ shown in Fig. 2. We see a $\sqrt{f}$ dependence at both low and high frequency, with a transition region near 1 kHz. In Fig. 3 we show the relative error in ¥ ; i.e.,

$$Rel.Error = \left| \frac{\mathrm{Re}(¥) - \mathrm{Re}\left(¥\right)}{\mathrm{Re}(¥)} \right| \quad . \tag{40}$$

The relative error is less than 0.3% at all frequencies from DC to 100 GHz, demonstrating the validity of the new approximate formulas for h_3 and ¥ .

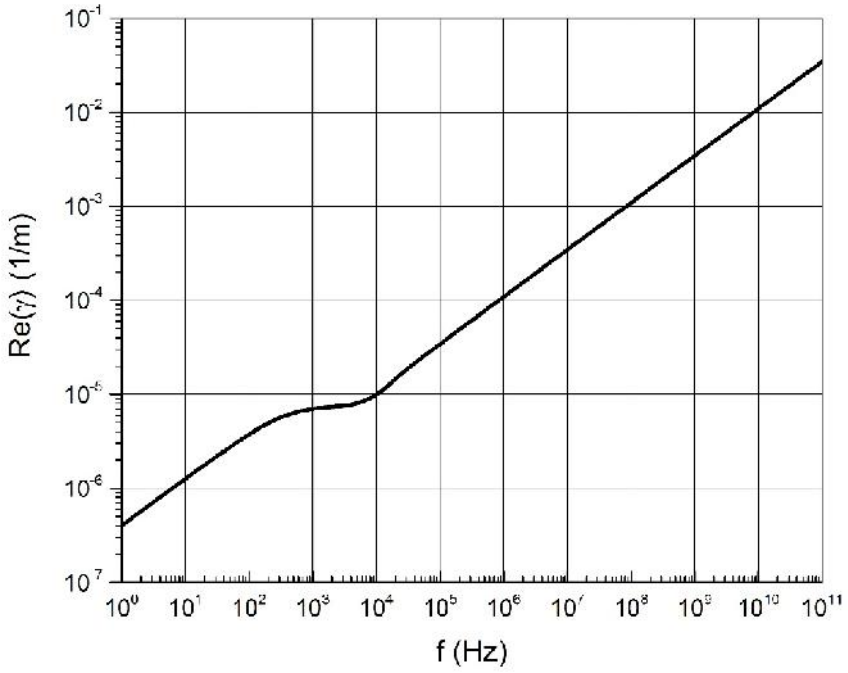

Figure 2. $Re(¥)$ from numerical solution of $det[\bar{\bar{M}}] = 0$.

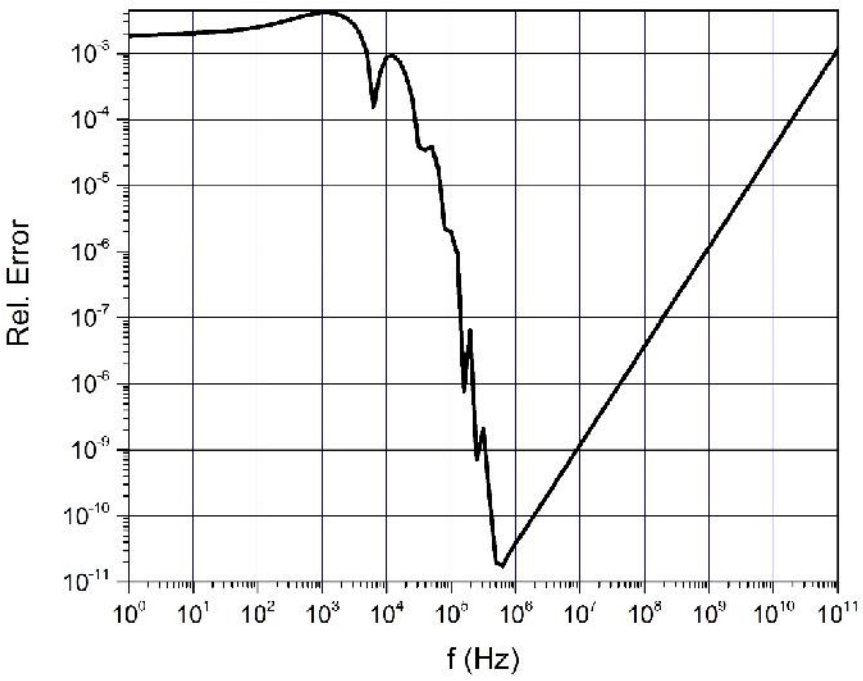

Figure 3. Relative error in $Re(¥)$.

4. Circuit Model for Lossy Coaxial Line:

It is well known that the simple circuit of Fig. 4 can be used to model a short section of lossy transmission line, length Δz (see, for example, pgs. 43-46 of Ref. [9]).

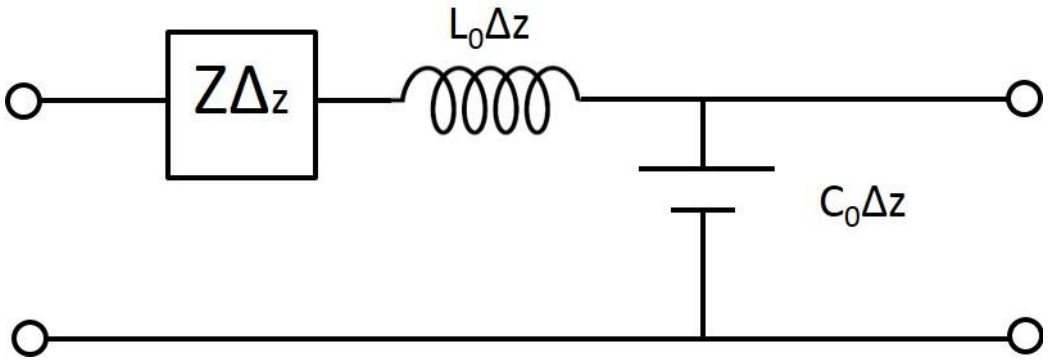

Figure 4. Circuit model for short section of transmission line.

The impedance Z models the frequency dependent dispersion and attenuation present in the line, in our case due to walls of finite conductivity. A number N of such sections are cascaded together to model a transmission line of finite length $L = N\Delta z$. The inductance L_0 and capacitance C_0 are given by

$$L_0 = \frac{«_0}{2®} log\left(a_2 / a_1\right) \text{ (H m}^{-1}\text{)} \tag{41}$$

$$C_0 = \frac{2\pi\epsilon_3}{\log\left(a_2 / a_1\right)} \quad (\text{F m}^{-1}) \tag{42}$$

We note that such a circuit (Ref. [9], pg. 46) produces a longitudinal propagation constant

$$\gamma^2 = \left[Z(\omega) + i\omega L_0\right](i\omega C_0) \tag{43}$$

(see Eq. 2.12 of Ref. [9]). We assume here that the shunt conductance is negligibly small.) Comparing Eqs. (38) and (43) gives

$$Z(\omega) = \frac{\omega\mu_0}{2\pi}\left[\frac{1}{k_2 a_1}\frac{F_4(h_2 a_1)}{F_2(h_2 a_1)} - \frac{1}{k_4 a_2}\frac{G_3(h_4 a_2)}{G_1(h_4 a_2)}\right] . \tag{44}$$

In terms of the Laplace Transform variable $s = i\omega$,

$$Z(s) = \frac{\eta_2}{2\pi a_1}\frac{F_4(h_2 a_1)}{F_2(h_2 a_1)} - \frac{\eta_4}{2\pi a_2}\frac{G_3(h_4 a_2)}{G_1(h_4 a_2)} , \tag{45}$$

where

$$\eta_i = \sqrt{\frac{s\mu_0}{\sigma_i}} , \quad \text{i=2,4} , \tag{46}$$

$$h_i^2 = -\gamma^2 + s^2\mu_0\epsilon_i + s\mu_0\sigma_i , \qquad \text{i=2,4} . \tag{47}$$

We note that as $s \to 0$, using small argument expansions for I and K,

$$\lim_{s\to 0} Z(s) = \frac{1}{\pi\left(a_1^2 - a_0^2\right)\sigma_2} + \frac{1}{\pi\left(a_3^2 - a_2^2\right)\sigma_4} . \tag{48}$$

We wish to find an electrical circuit which has the above impedance [Eq. (45)] for our model. Following the analysis of Ref. [10], we arrive at the equivalent circuit shown in Fig. 5.

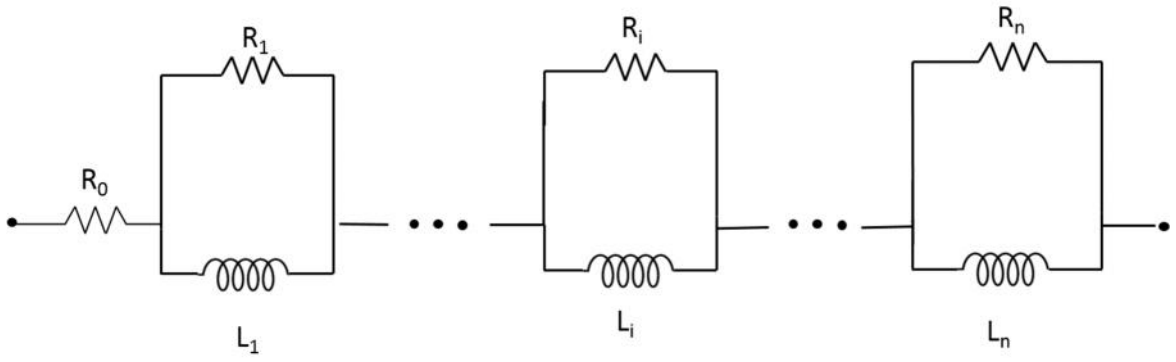

Figure 5. Equivalent circuit model for impedance Z(s) of Eq. (45) where $i = 1..n$.

The resistor R_0 insures the proper $s \to 0$ limit, and the subsequent circuit elements are chosen to give the correct frequency dependence of the impedance. Benchmark calculations with $n = 8$ are included in Sec. 6.

5. Benchmark FDTD Simulations

The Chicago FDTD code was used to conduct fully electromagnetic 2D (r, z) simulations of a coaxial transmission line with finite conductivity walls. Figures 1 and 6 illustrate the geometry schematically, and the dimensions and parameters are as in Eqs. (39). The conductivity was dropped to $\pm = 10^{14}\ \text{s}^{-1}$ so as to make resolution of the skin depth in the walls manageable. The simulated transmission line configuration was started and ended with one cm of a perfect electrical conductor (PEC) line to simplify the connection input and output boundary conditions. The cell sizes were set at $dr = 1.0 \times 10^{-3}$ cm and $dz = 4.0 \times 10^{-3}$ cm. The outer radial boundary was placed 3 cm beyond the outer radius of the coaxial line. A metal boundary here had negligible effect on signal propagation in the coaxial line.

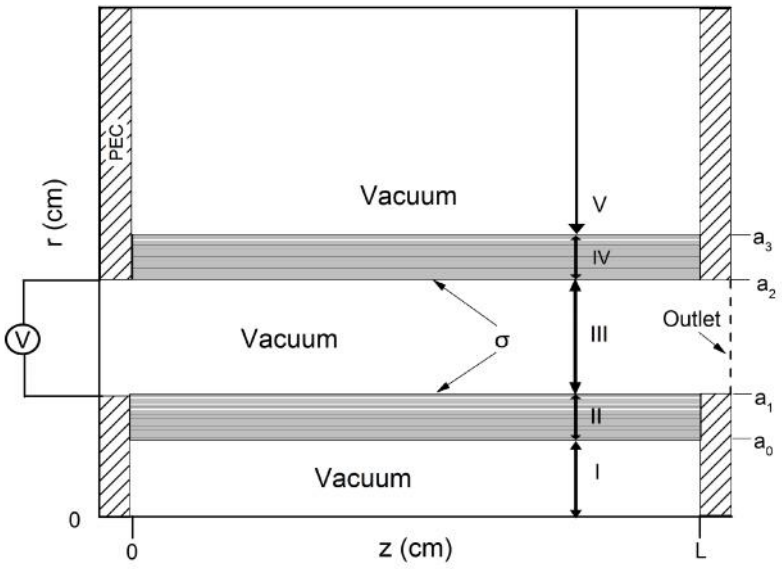

Figure 6: Schematic of the FDTD Chicago simulation.

For single frequency runs of 10^9 and 10^{10} Hz the length of the lossy line was set to L=40 cm and L=20 cm, respectively. For 10^9 Hz, the $Re(¥)$ from Eq. (21) is 0.243 m^{-1} giving an attenuation of $e^{-0.243(0.4)} = 0.907$. The attenuation measured from the Chicago simulation agreed to three significant figures. At 10^{10} Hz, $Re(¥) = 0.772 m^{-1}$ and the corresponding attenuation is $e^{-0.772(0.2)} = 0.857$. Again, the Chicago simulation result agreed to three significant figures. A final simulation with a short pulse flat-top voltage input and length L=80 cm was run. Figure 7 shows the input pulse and the attenuated and distorted output voltage. All these results are compared to results from circuit model calculations in the next section.

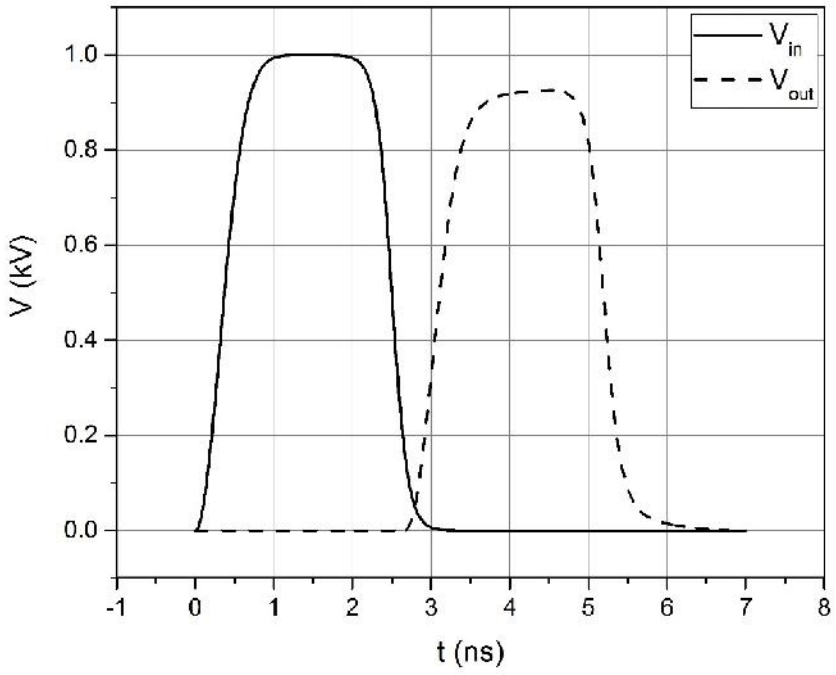

Figure 7. Short pulse voltage input and voltage output from FDTD simulation.

6. Circuit Model Calculations:

In this section we report on signal attenuation calculations using the circuit model described in Sec. 4. The model was benchmarked against the numerical and analytic results of Secs. 2 and 3 as well as the FDTD simulations of Sec. 5.

The first set of calculations corresponds to the parameters of (39) but with $\pm_2 = \pm_4 = 10^{14}$ s^{-1} which were used in the FDTD simulations. The circuit model parameters shown in Table 1. were obtained by performing a least squares fit to the impedance formula of Eq. (45). Overlay of the fit to Eq. (45) is shown in Fig. 8 – the maximum error in the fits is <0.1% and not visible in the figure. For this first set of calculations we used $\Delta z = 0.001$ m. The circuit consists of a large number N of blocks to give the desired length of transmission line, $L = N\Delta z$. The coupled differential equations which represent the complete circuit were solved using a 4th order Runge Kutta solver with time step $\Delta t = 5.0 \times 10^{-13} s$ dictated by the circuit parameters of Table 1. Results from a series of three single frequency voltage input runs are summarized in Table 2. Attenuation values calculated using ¥ from Eq. (21), ¥ˆ from Eq. (38), FDTD simulation, and circuit model calculations all agree to better than 1%. The circuit model was also used to calculate the attenuation of the short, flat-top voltage input pulse of Fig. 7. The output pulse is shown in Fig. 9 and is in excellent agreement with the FDTD result.

n	R_n	L_n
0	3.19154209	-
1	5.05066329E-06	3.54496414E-06
2	7.61995142E-05	2.62321493E-07
3	6.63213346	9.11242933E-09
4	15.9945196	8.95067161E-10
5	142.329675	3.87129052E-10
6	1153.13619	2.11040256E-10
7	44.3915849	7.41266698E-10
8	13.0879065	2.92021043E-09

Table 1. Circuit model parameters for $\pm_2 = \pm_4 = 10^{14}$ s^{-1} and geometry as in (39).

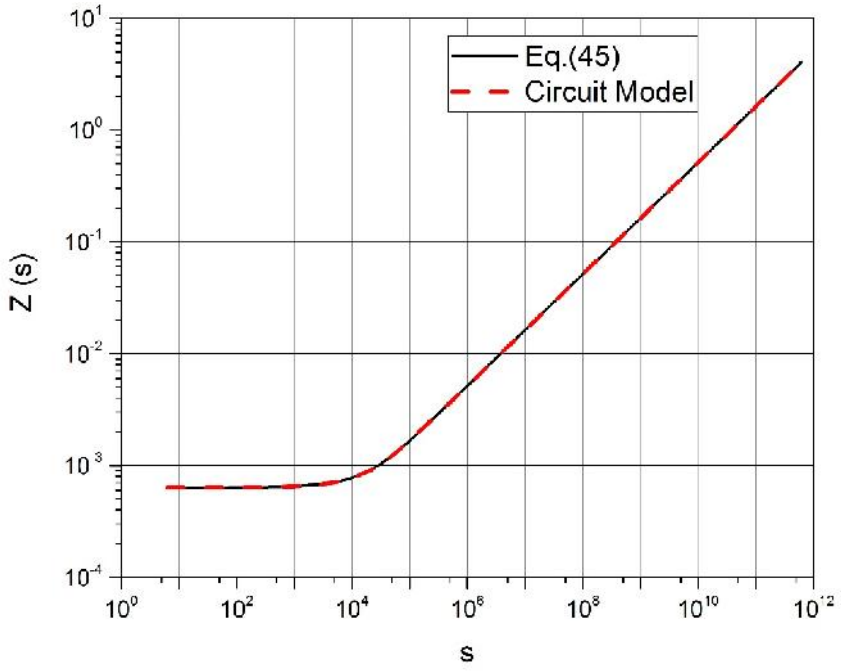

Figure 8. Z(s) from Eq. (45) and circuit model fit for $\pm_2 = \pm_4 = 1.0x10^{14}\,s^{-1}$.

	f(Hz)	L(m)	$e^{-¥L}$	$e^{-¥L}$	FDTD Attenuation	Circuit Mod. Attenuation
1	10^8	3.0	0.804	0.803	-	0.799
2	10^9	0.4	0.907	0.906	0.907	0.906
3	10^{10}	0.2	0.857	0.856	0.857	0.851

Table 2. Attenuation of single frequency signals in coaxial line ($\pm_2 = \pm_4 = 10^{14}$ s^{-1}).

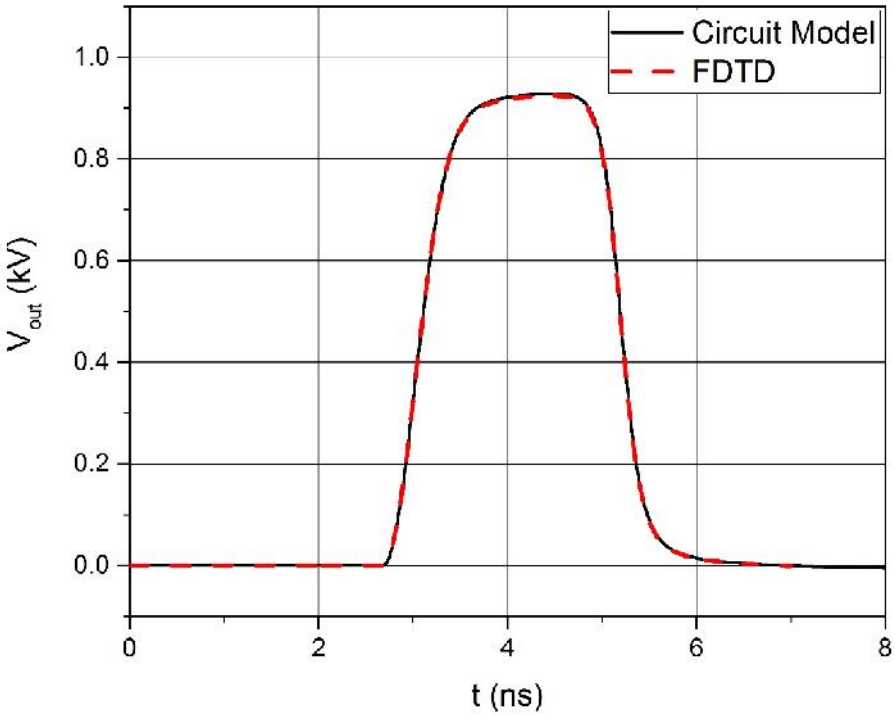

Figure 9. Output voltages from FDTD simulation and circuit model calculation.

The circuit model calculations described above were repeated for $\pm_2 = \pm_4 = 5.0\times10^{17}$ s^{-1} (high conductivity metal). The corresponding model parameters are shown in Table 3, and the fit to $Z(s)$ is shown in Fig. 10 – maximum error in the fit is <1% and again not visible in the overlay. Agreement with numerical and analytic results shown in Table 4 is again excellent (FDTD simulations at this high conductivity were impractical). The short pulse voltage output at $L = 50$ m is shown in Fig. 11. The shape of the output pulse shows the same tilting of the flat-top observed in the calculations for $\pm = 10^{14}$ s^{-1}.

n	R_n	L_n
0	6.383084E-04	-
1	9.1270945E-03	2.2475216E-09
2	2.3432059E-03	1.0747672E-08
3	2.2109079E-01	4.71494072E-11
4	8.6811974E-02	1.47303812E-10
5	1.5852013	7.11164226E-12
6	12.6009311	3.82817718E-12
7	5.5375742E-01	1.72513781E-11
8	3.0723828E-02	5.40384424E-10

Table 3. Circuit Model Parameters for $\pm_2 = \pm_4 = 5.0x10^{17}\,s^{-1}$ and geometry as in (39).

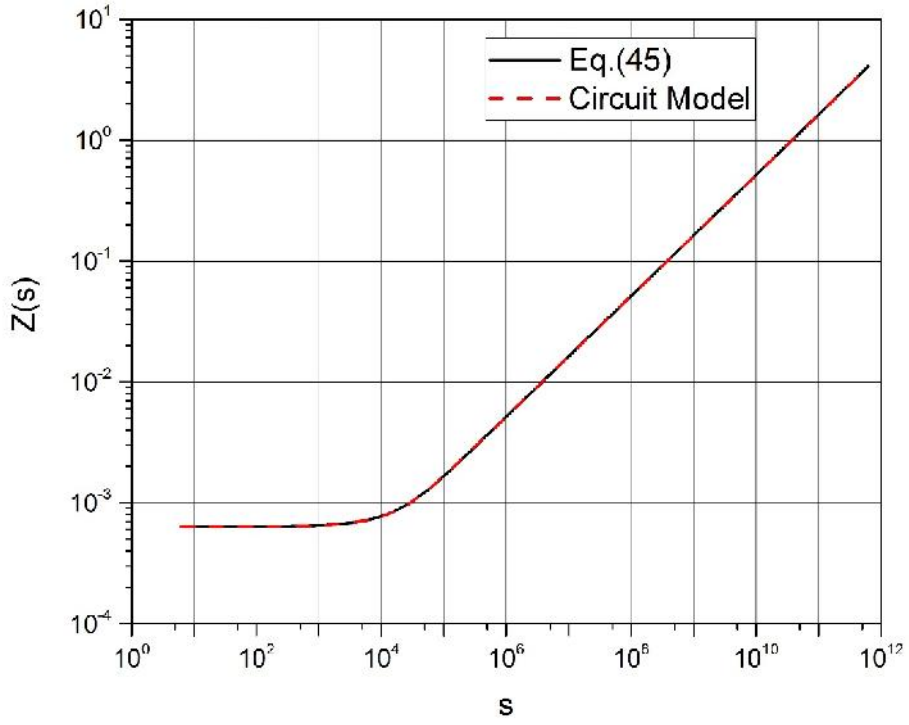

Figure 10. Z(s) from Eq. (45) and circuit model fit for $\pm_2 = \pm_4 = 5.0\times10^{17}\,s^{-1}$.

	f(Hz)	L(m)	Δz (m)	$e^{-¥L}$	$e^{-¥L}$	Circuit Mod. Attenuation
1	10^8	100	0.01	0.897	0.895	0.894
2	10^9	30	0.003	0.900	0.900	0.899
3	10^{10}	10	0.001	0.897	0.896	0.898

Table 4. Attenuation of single frequency signals in coaxial line ($\pm_2 = \pm_4 = 5.0\times10^{17}\,s^{-1}$).

7. Summary

New approximate analytic formulas have been derived for the impedance and attenuation constant of a lossy coaxial transmission line. These general formulas reduce to previously derived results in the appropriate limits. Accuracy of the formulas from DC to 100 GHz was established by comparison to numerical solutions based on the exact field equations. A new circuit model was also derived in which the line impedance is represented by a series of resistor-inductor loops. Model results were shown to be in excellent agreement with the numerical and analytic results, and were also benchmarked against FDTD electromagnetic simulations which resolved the conductor skin-depths. The model allows for fast calculation in a general transmission line code, or as part of a larger circuit model which makes use of standard differential equation solution methods.

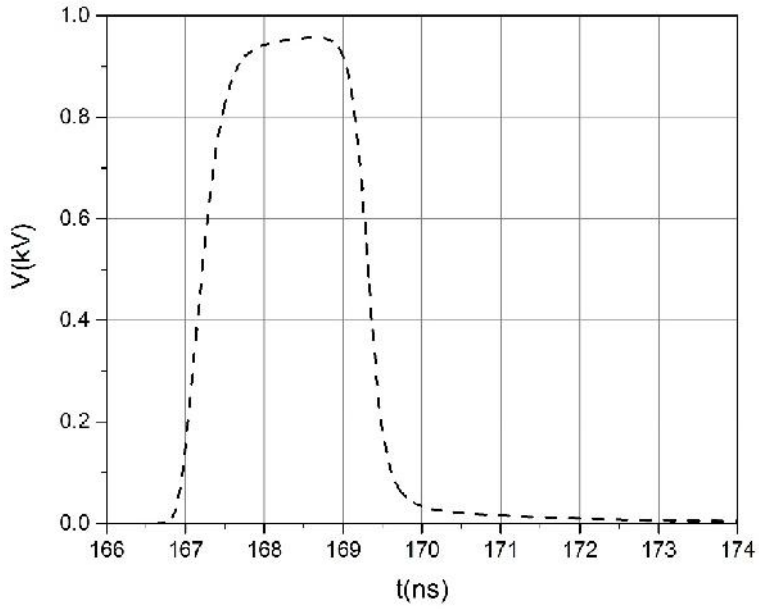

Figure 11. Short pulse voltage output with $\pm = 5.0\times10^{17}\,s^{-1}$ at L=50m from circuit model calculations.

Acknowledgments

The authors would like to thank W. A. Stygar, B. T. Hutsel, J. J. Leckbee, T. Webb, and M. Kiefer at Sandia for helpful discussions regarding this research. This work was supported by Sandia National Laboratory. Sandia is a multiprogram laboratory operated by Sandia Corporation, a Lockheed Martin Company, for the National Nuclear Security Administration under DE-AC4-94AL85000.

References

1. E.Tuncer, B.T. Lee, S. Islam and D.P. Neikirk, IEEE Trans. Microw. Theory Techn., 42, 9 (1994).
2. S. Schelkunoff, Bell System Technical Journal 13, 532 (1934).
3. J.A. Stratton, Electromagnetic Theory, McGraw-Hill: New York, 1941.
4. W.C. Daywitt, IEEE Trans. Microw. Theory 38, 1313 (1991).
5. M.I. Gallant, http://www.jensign.com/RG58U/fields.html.
6. C.R. Paul, IEEE Trans. Electromagn. Compat. 36, 2 (1994).
7. R.L. Wigington and N.S. Nahman, Proc. IRE 45,166 (1957).
8. C. Yen, Z. Fazarinc and R. L. Wheeler, Proc. IEEE 70, 7 (1982).
9. P.W. Smith, Transient Electronics Pulsed Circuit Technology, John Wiley and Sons: Hoboken, NJ, 2002.
10. T.C. Genoni, D.V. Rose, R.E. Clark, D.R. Welch and W.A. Stygar, Phys. Rev. ST Accel. Beams 15, 010401 (2012).